I.A.U. Karaj Branch

Journal of Applied Chemical Research, 11, 1, 95-106 (2017)

Journal of Applied Chemical Research
www.jacr.kiau.ac.ir

Gel-Citrate Method for Fabrication of Nano $La_{0.7}Sr_{0.3}MnO_3$ Perovskite Type Oxide and its Application in Removal of RB4 Dye

Haman Tavakkoli*, Farideh Sarafion

Department of Chemistry, Ahvaz Branch, Islamic Azad University, Ahvaz, Iran

(Received 17 Jul. 2016; Final version received 19 Sep. 2016)

Abstract

In this work $La_{0.7}Sr_{0.3}MnO_3$, one group of nanosized perovskite-type oxides were prepared by sol-gel method. The perovskite structure has been characterized by X-ray diffraction (XRD) , scanning electron microscopy (SEM) , energy dispersive X-ray spectrometer (EDX) and Fourier transform infrared (FTIR) . The nanoparticles showed the excellent adsorption properties towards reactive blue 4 (RB4) as a reactive dye. The adsorption studies are carried out at different pH values, different adsorbate concentrations, various adsorbent dosages, different temperature, and contact time in a batch experiments to find the optimum conditions.

Keywords: *Perovskite, sol-gel method, Nanoparticle, Dye, Reactive Blue 4.*

Introduction

The family of perovskite-type oxides generally formulated as ABO_3 (A is a rare earth metal with large ionic radius or alkali earth metals; B is a transition metal with a small ionic radius) Significant catalytic applications of these perovskites include reactors for partial and total oxidation of hydrocarbons and in devices for the removal of pollutants from combustion gases [1,2] and could be considered as an adsorbent /catalyst material for the removal of dyes [3,4].

Dye effluents from textile industries and photographic industries are becoming a serious environmental problem because of their toxicity, unacceptable color, high chemical oxygen demand content, and biological degradation [5]. Dyes can be classified as anionic (direct, acid, and reactive dyes), cationic (basic dyes) and non-ionic(disperse dyes) [6]. Waste waters offer considerable resistance for their biodegradation due to presence of these heat and light stable dyes, thus upsetting aquatic life [7]. Several treatment methods including

***Corresponding author:** Haman Tavakkoli, Department of Chemistry, Ahwaz Branch, Islamic Azad University, Ahwaz, Iran. Tel: +98 613 4457612, Fax: +98 613 4435288. E-mail: htavakkoli59@gmail.com.*

coagulation, chemical oxidation, membrane separation and adsorption techniques have been proposed for the treatment of dye waste water. Considerable amounts of the literature reports the adsorption of dyes on various adsorbent surfaces especially nanomaterials [8, 9].

The first aim of the present study is to fabricate and characterize of perovskite-type oxide nanoparticles $La_{0.7}Sr_{0.3}MnO_3$ (LSMO). Investigation of the efficiency of the perovskite-type oxide nanoparticles as adsorbent for the removal of Reactive Blue4 dye (RB4), from aqueous solutions is the second goal and to explain the adsorption of RB4 onto nanoparticles $La_{0.7}Sr_{0.3}MnO_3$using isotherm models.

Experimental

Reagents

$La(NO_3)_3.6H_2O$ (99.99% purity), $Sr(NO_3)_2$ (99.99% purity), $(CH_3COO)_2Mn.4H_2O$ (99.99% purity) were all obtained from Merck, Germany; citric acid (CA) (99.5% purity), was purchased from Aldrich, USA. The commercial color index (CI) diazo dye (RB4, molecular weight = 681.39 g/mol) was generously provided by Sigma company, T8154-20ml USA which was used without further purification (Figure 1). All the reagents were of analytical grade and thus used as received. Deionized water was used throughout the experiments.

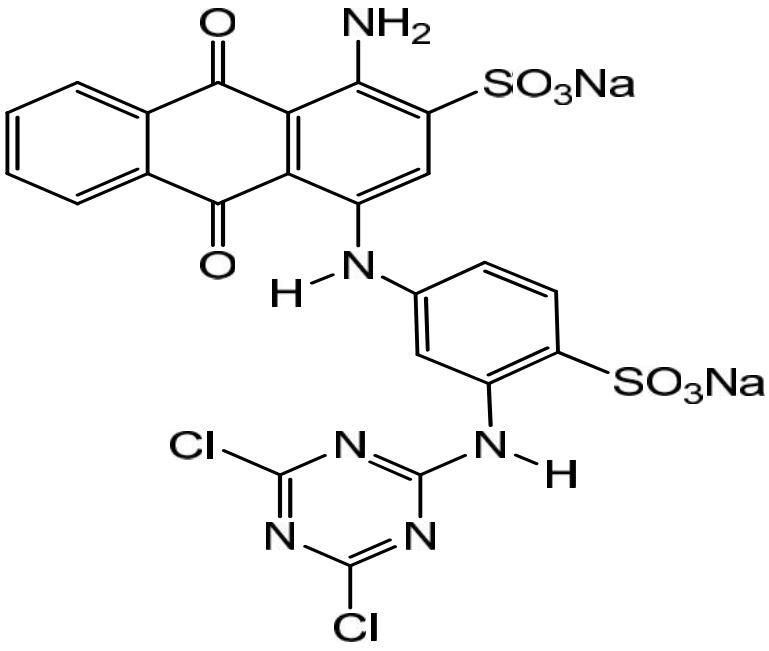

Figure 1. Molecular structure ofReactive Blue 4 (RB4) dye.

Preparation and characterization of $La_{0.7}Sr_{0.3}MnO_3$

For the preparation of the nanoperovskite in this work, Proportional amounts of, $La(NO_3)_3.6H_2O$, $Sr(NO_3)_2$ and $(CH_3COO)_2Mn.4H_2O$, were dissolved in 20 ml of deionized water, Citric acid (CA) was proportionally added to the metal solution by stirring at room temperature. The solution was concentrated by evaporation at approximately 75°C to remove excess water. Then, the dry gel was obtained by letting the sol into an oven and heated slowly up to 110°C and kept for 10 h in baking oven. Then, it was ground in agate mortar and turned into powder and calcinated at 750°C in air for 9 h. The annealing of the amorphous precursor allows removing most of the residual carbon and the orthorhombic perovskite phase was obtained.

The complex polymeric gel and derived powders have been also analyzed by Fourier transform infrared (FTIR) spectroscopy on Perkin Elmer BX II FTIR spectrometer. The crystallization and microstructure of the oxide powders have been characterized with an X-ray diffractometer employing a scanning rate of 0.02 S^{-1} in a 2θ range from 20 to 70°, using a Ý pert, 200, Equinox 3000, France, equipped with CuKα radiation. The data have been analyzed using JCPDS standards. The microstructure and elemental distribution on the surface were investigated using KYKY EM3200 (V=30kV) scanning electron microscopy and energy dispersive X-ray spectroscopy (EDX, Inca 400, Oxford Instruments). A UV–Vis spectrophotometer (Perkin Elmer lambda 35) was employed to monitor adsorption of dyes.

Dye removal experiments

A prepared solution ofRB4 was distributed into different flasks (1 L capacity) and pH was adjusted with the help of the pH meter (HORIBA F 11 E, Japan made). The initial pH value of the dye solution was adjusted to the desired levels, using either HCl (0.5 M) or NaOH (0.5 M). A known mass of nano-LSMO powder (adsorbent dosage) was then added to 10 mL of the RB4 aqueous solution, and the obtained suspension was immediately stirred for a predefined time. All experiments were done at the room temperature. The investigated ranges of the experimental variables were as follows: dye concentration (50-300 mg/L), pH of solution (1-13), adsorbent dosage (0.005, 0.01and 0.02) and mixing time (1- 30 min). After a preselected time of decolorization, samples were collected and absorbance of the solution at a λ_{max} equals to 595 nm was measured to monitor the residual RB4 concentration.

Results and Discussion

X-ray Diffraction

XRD patterns of the synthesized nanopowder which calcined at 700°C for 9 h (heating rate:

3°C/min) is shown in Fig. 2. XRD results reveal the existence of a perovskite-type phase for sol-gel method at this temperature. When the precursor was calcined at 700°C for 9 hours, several sharp peaks were observed attributed to the perovskite $La_{0.7}Sr_{0.3}MnO_3$ by comparison with standard XRD spectra. The diffraction peaks at 2θ angels appeared in the order of 23.44°, 33.72°, 41.08°,47.88°and 59.68° can be assigned to scattering from the (0 2 1), (1 1 0), (2 0 2), (2 0 4)and (4 2 1) planes of the $La_{0.7}Sr_{0.3}MnO_3$ perovskite type crystal lattice, respectively]10].

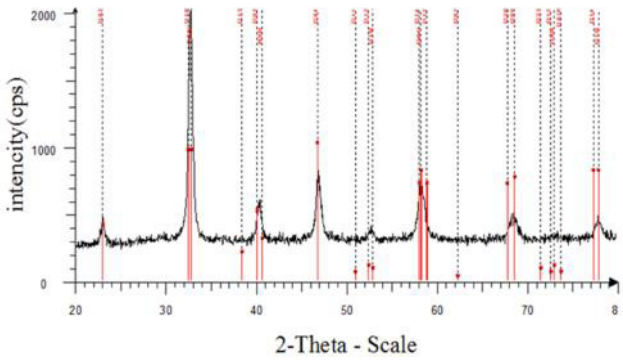

Figure 2. XRD patterns of samples of the LSMO nanopowder calcinated at 700°C.

XRD data also shows $La^{0.5}Ca^{0.5}FeO^3$ crystallizes in a hexagonal phase with a = 5.523, b = 5.523, c = 13.324 Å. The crystallite sizes were calculated using XRD peak broadening of the (1 1 0) peak using the Scherer's formula (1):

$$D_{hkl} = \frac{0.9\lambda}{\beta_{hkl}\cos\theta_{hkl}} \quad (1)$$

where Dhkl is the particle size perpendicular to the normal line of (hkl) plane, βhkl is the full width at half maximum, θ_{hkl} is the Bragg angle of (hkl) peak, and λ is the wavelength of X-ray. The particle sizes of LSMO nanoparticles calcinated at 700°C is about 16.31 nm.

SEM and EDX Analysis

The surface and textural morphology of LSMO nanopowder by SEM image is illustrated in Fig. 3. According to the SEM image, the size of LSMO particles was found to range between 26 to 32 nm. The surface looks scaly and nearly fully covered with the particles that have grown on it. Moreover, the porosity of the surface is evident and it seems that the particles have grown with uniform size. The pores size varied from 0.1 to 0.3 μm. It must be mentioned that pores with large geometric dimensions are more suitable for water treatment. Also, the existence of these meso-pores facilitates the sorption of hazardous chemicals to the surface. This phenomenon

improved the efficiency and workability of LSMO as a promising adsorbent.

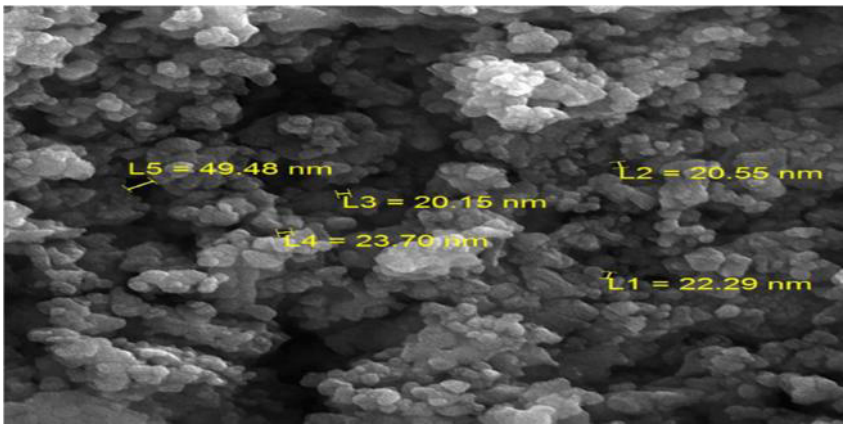

Figure 3. SEM images of LSMO nanopowders.

The EDX analysis was performed to further confirmation of the obtained product composition. Figure 4 Shows EDX spectrum which indicates the existence of La, Sr, Mn and O elements in this nanoparticle. Calculated composition for $La_{0.7}Sr_{0.3}MnO_3$; La:35.91, Ca:10.33, Fe:28.94 and O: 24.80, Found; La: 35.75, Ca:10.86, Fe:29.20 and O: 25.12.

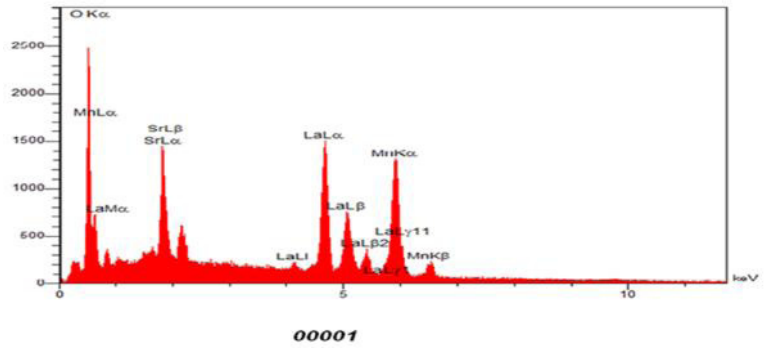

Figure 4. Energy dispersive X-ray (EDX) spectrum of the LSMO nanoparticles.

FT-IR Spectroscopy

The FT-IR spectra of the LSMO fresh xerogel and calcinated xerogel in the range of 500-4000 cm^{-1} were shown in Figure 5 (a,b). The dried gel of the sample shows the characteristic bands at about 1725, 1617 and 1385 cm^{-1} corresponds to the symmetric and anti-symmetric stretching mode of carboxylate group [11,12]. The band at about 1230 cm^{-1} assigned to the NO3 stretching vibration [13]. The absorption band around 1080 cm^{-1} is attributed to C–O bond [14]. As can be seen in Fig.5 b, the bands correspond to O–H group, NO_3, and carboxylate ligand disappears as the gel was calcinated at 700°C. This indicates the possibility of metal carboxylate dissociation

and conversion to metal oxides during the calcinations process. Also, the observed peak at about 580 cm^{-1} is due to the stretching internal vibrations of octahedral oxygen in perovskite oxide structure.

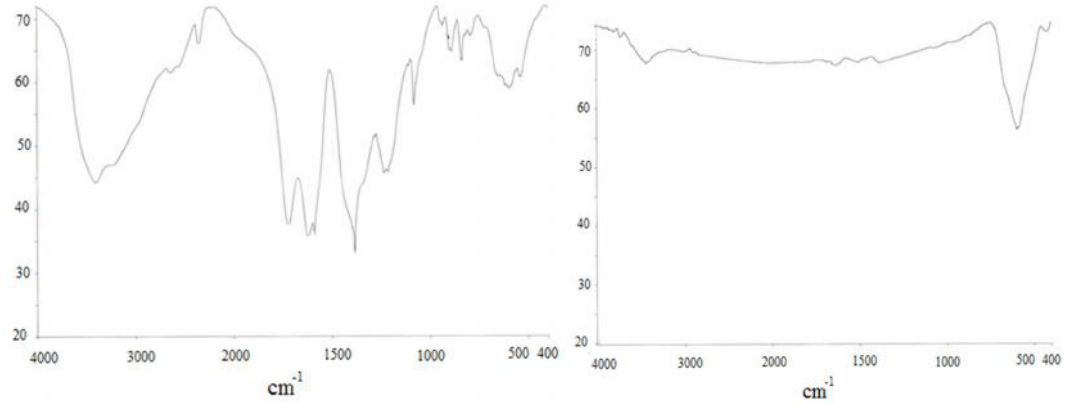

a **b**

Figure 5.FT-IR spectra of LSMO precursor (a), and the calcinated powders at 700 °C (b).

Adsorption experiment

The efficiency of the prepared and characterized LSMO nanoparticle as an adsorbent for removal of RB4 from liquid solutions was investigated using a batch equilibrium technique placing different amount of adsorbent in a glass bottle containing 10 ml of a dye solution at 50 mg/L concentrations. The adsorption studies were carried out for different pH values; contact time, adsorbent dosage and dye solution concentrations and results are presented in the following sections.

Effect of pH

Solution pH is an important parameter that affects adsorption of dye molecules. The effect of the initial solution pH on the dye removal efficiency of RB4 by LSMO nanoparticles was evaluated at different pH values, ranging from 1 to 13, with a stirring time of 30 min. The initial concentrations of dye and adsorbent dosage were set at 50 mg/L and 0.01 g, respectively. The percentage of dye removal is defined as (2):

$$\text{Removal rate \%} = \frac{C_o - C(t)}{C_o} \times 100 \quad (2)$$

where C0 and $C(_t)$ are the initial concentration and concentration of RB4 at time t, respectively. As shown in Figure 6, the dye removal was much higher in acidic pH (pH 1 and 2), and decreased when the pH was increased from 3 to 13. Since the removal of RB4 increased to its maximum value at pH 2 (the removal of RB4 above 94% was achieved) the electrostatic attraction between the dye molecules (negatively charged) and LSMO surface (positively charged) might be

the predominant adsorption mechanism [15]. Therefore, to have the optimized condition to remove RB4, acidic pH should be applied and pH 2 seems to lead to the best result; so this pH was selected to run further experiments.

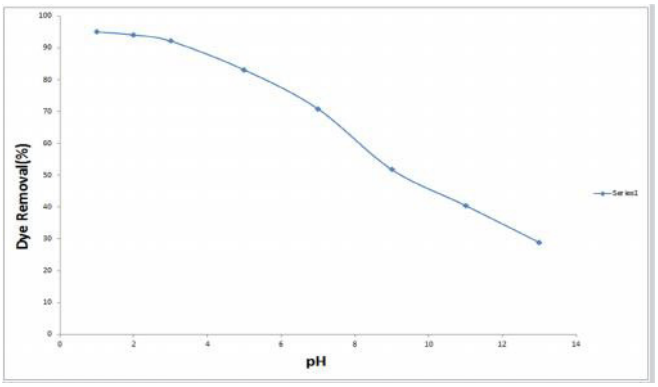

Figure 6. Effect of initial pH of dye solution on removal of RB4 (LSMO dosage = 0.01 g, initial dye concentration = 50 mg/L, stirring time = 20 min).

This is likely attributed to the fact that an acidic pH causes the LSMO adsorbent surface to carry more positive charges and thus would more significantly attract the negatively charged species (dye molecules) in solution and enhanced its electrostatic attraction for dye adsorption. Therefore the lower adsorption of Trypan blue at higher pH values resulted from an increased repulsion between the more negatively charged dye species and negatively charged active sites on surface.

Effect of contact time and adsorbent dosage

To further assessing of dye removal, the effects of contact time and adsorbent concentration on the removal of RB4 by LSMO nanoparticles were examined. Initial dye concentrations and pH of the solutions were fixed at 50 mg/L and 2, respectively, for all the batch experiments. Results are shown in Figure 7. As indicated, increasing of contact time in different dosages of adsorbent led to decrease in the concentration of RB4. This behavior was also observed when adsorbent dosage increased from 0.005 to 0.02 g. This decreasing in the concentration is due to the adsorption of RB 4on LSMO nanoparticles and the greater number of adsorption sites for dye molecules made available at greater LSMO dosages]17,18[. The removal efficiency of RB4at the initial dosage of 0.01 g, increased from 91.86% at the second minute of contact to 96.45% at time equals to 30 min by keeping constant stirring, however, with increasing LSMO dosage to 0.02 g the percentage of removal obtained in the second minute of stirring was 90.48%, and the most percent of removal (92.91%) was attained when the stirring was continued till

time equals to 15 min. The adsorbent dosage obtained in this study for complete removal of RB4 on to LSMO nanopowder is less than most of the reported values in the literatures for dye adsorption using other adsorbents [18-21].

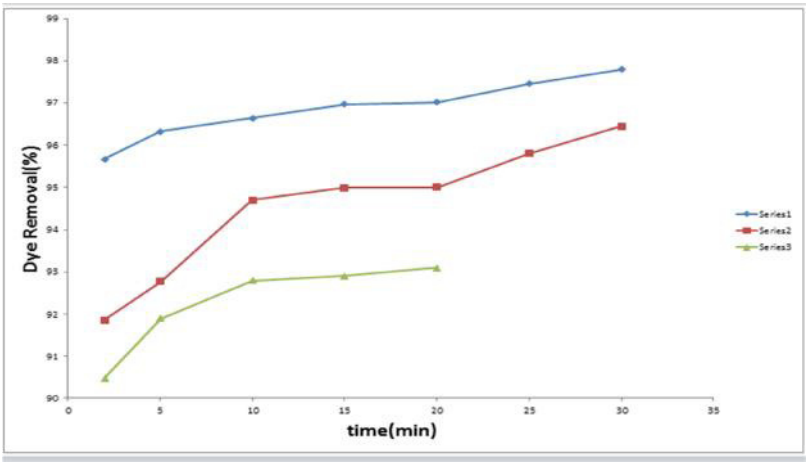

Figure 7. Effect of stirring time on removal of RB4 in different doses of LSMO (initial dye concentration = 50 mg/L, initial pH 2).

Effect of dye concentration

The initial dye concentration is another important variable that can affect the adsorption process. The effect of initial RB4 concentration on dye removal efficiency by LSMO particles was studied by varying the initial dye concentration from 50 to300 mg/L at pH 2, an adsorbent dosage of 0.01g and contact time of 20 min, as shown in Fig. 8. Results show that decolorization of textile dyeRB4 decreases with increasing initial concentration. As it is obvious, the percentage removal of RB4 decreased from around 94% at a concentration of 50 mg/L to 84% when the concentration was increased to 300 mg/L. This behavior reveals the dependency of adsorption to initial concentration of RB4.

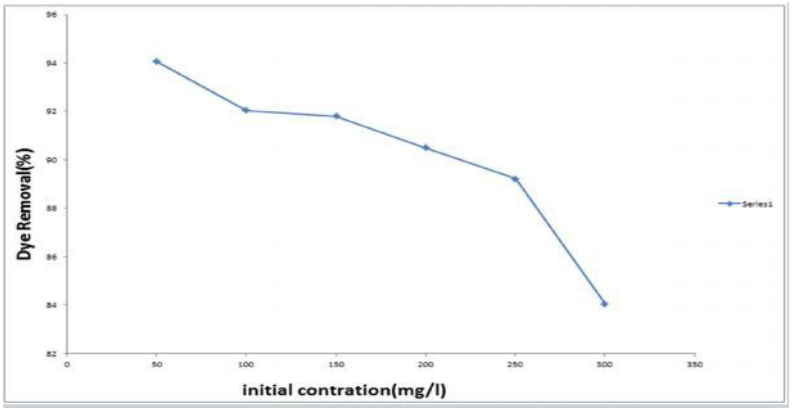

Figure 8. Effect of initial dye concentration on removal of RB4 (LSMO dosage = 0.01 g, initial pH 2, stirring time = 20 min).

Adsorption kinetic studies

To find the suitable chemical removal model for describing the experimental kinetic data, the obtained data were evaluated using pseudo-first and pseudo-second-order reaction rate models [22,23].

For the pseudo-first and pseudo-second order kinetic model, the experimental data have been fitted with the following equations:

Pseudo-first-order equation: $\log(qe - qt) = \log qe - (\frac{k_1}{2.3}t)$ (3)

Pseudo-second-order equation: $\frac{t}{q_t} = \frac{1}{k_2 q_e^2} + \frac{1}{q_e}$ (4)

where k_1 and k_2 are the first-order and second-order rate constant, respectively; C_0 stands for the initial RB4 concentration and C(t) is the concentration of RB4 at time t. Higher value of R^2 were obtained for pseudo-first-order (0.98) than for pseudo-second-order (0.99) adsorption rate models, indicating that the adsorption rates of RB4 on to the LSMO nanoparticles can be more appropriately described using the pseudo-first-order rate rather than pseudo-second-order rate. The values of the rate constant, k_1 and k_2 are 0.104 and 0.154 (M^{-1} min^{-1}), respectively.

Adsorption isotherms studies

The equilibrium isotherm of a specific adsorbent represents its adsorptive characteristics and analysis of isotherm data is so important to predict the adsorption capacity of the adsorbent, which is one of the main parameters required for designing the adsorption processes [24].

The amount of dye adsorbed onto LSMO nanoparticles has been calculated based on the following mass balance equation:

$$q_e = \frac{V(C_0 - C_e)}{m} \quad (5)$$

Where q_e is equilibrium dye concentration on adsorbent (mg/g), V is the volume of the dye solution (L), C_0 and C_e (mg/L) are the initial and equilibrium dye concentrations, respectively, and m (g) is the mass of LSMO nanoparticles. Figure 9.shows the changes of q_e versus C_e which describes the interactive behavior between adsorbate and adsorbent.

Various isotherm models, such as Langmuir, Freundlich, and Temkin were applied to describe the nonlinear equilibrium relationship between the solute adsorbed onto the adsorbent and that left in the solution. An adsorption isotherm is characterized by certain constants which values express the surface properties and affinity of the adsorbent.

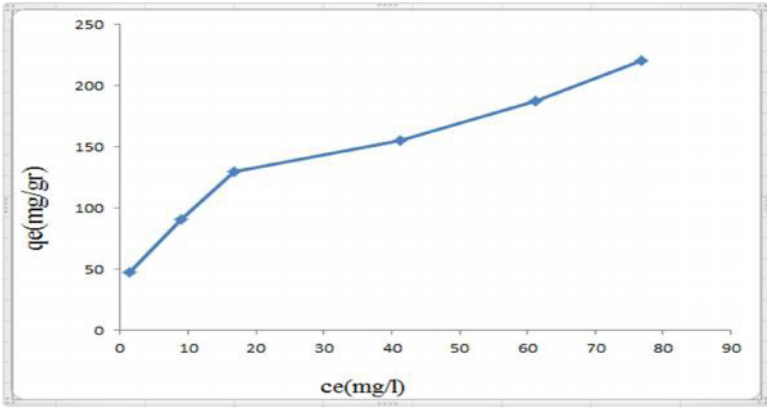

Figure 9. Plots of qe vs. Ce for removal of RB4 (LSMO dosage=0.01 g, initial dye concentration, 50, 100, 150, 200,250 and300 mg/L, volume of dye solution=10 mL, stirring time=20 min, initial pH 2).

The Langmuir model equation, assuming monolayer adsorption on a homogeneous adsorbent surface, can be presented as follows [25]:

$$\frac{C_e}{q_e} = \frac{1}{K_L q_{\max}} + \frac{C_e}{q_{\max}} \qquad (6)$$

where the q_{max} (mg/g) is the surface concentration at monolayer coverage which illustrates the maximum value of q_e and it can be attained as C_e is increased. The values of qmax and K_L can be determined from the linear regression plot of (C_e/q_e) versus C_e.

The linearized form of the Freundlich isotherm is expressed as follows [26]:

$$\log q_e = \log K_F + \frac{1}{n} \log C_e \qquad (7)$$

where K_F and n are constants of the Freundlich equation. The constant K_F represents the capacity of the adsorbent for the adsorbate and n is related to the adsorption distribution. A linear regression plot of log q_e versus log C_e gives the K_F and *n* values.

The derivation of the Temkin isotherm assumes that the fall in the heat of adsorption is linear rather than logarithmic, as implied in the Freundlich equation. The Temkin isotherm is as following:

$$q_e = A + B \ln C_e \qquad (8)$$

where A and B are isotherm constants [27].

Table 1. Isotherm constants for RB4 adsorption on LSMO nanoparticles.

Adsorbent	**Langmuir model**			**Freundlich model**			**Temkin model**		
$La_{0.7}Sr_{0.3}MnO_3$	q_{max} (mg g^{-1})	b (L mg^{-1})	R^2	K_f($mg^{1-1/n}$ $L^{1/n}$ g^{-1})	n	R^2	A_T (L/g)	B_T (j/mol)	R^2
	232.558	0.083	0.9603	42.96	2.745	0.9898	62.30	1.787	0.9287

The experimental results of this study were fitted to the aforementioned models. The calculated adsorption parameters and correlation coefficient (R2) for the three isotherm models by linear regression are listed in Table 1. The value of correlation coefficient (R2) for Langmuir isotherm is greater than that of the Freundlich and Temkin isotherm for the adsorption of investigated dye. This indicates that the adsorption of RB4 on LSMO nanoparticles is better described by the Freundlich model than the others and generally it has been found better suited for characterizing monolayer adsorption process onto the homogeneous adsorbent surface. The linearized form plot of theFreundlich isotherm is shown in figure 10.

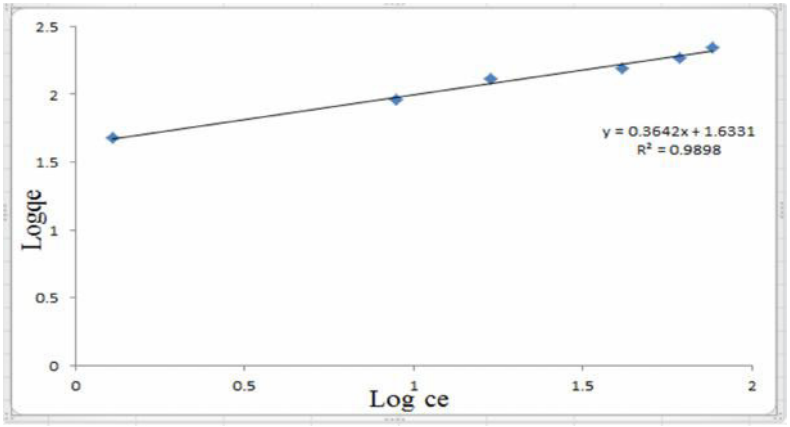

Figure 10. Freundlich isotherm plot of RB4 adsorption onto LSMO nanoparticles: LSMO dosage=0.01 g, initial pH 2, stirring time=20 min, initial dye concentration=50, 100, 150, 200, 250,300 mg/L.

Conclusion

In this study, a nanoparticle $La_{0.7}Sr_{0.3}MnO_3$ (LSMO) powder was produced and tested as a novel adsorbent for the removal of diazo dye. A systematic study on the structural, morphological and adsorption properties of $La_{0.7}Sr_{0.3}MnO_3$ samples has been carried out by means of various analytical techniques. Crystallization of orthorhombic phase LSMO occurs at 700°C. The effects of LSMO dosage, initial pH, contact time and initial dye concentration on the removal of RB4 was investigated through batch experiments. Results indicated that the synthesized powder could effectively remove high concentrations of diazo dye in a short contact time. The optimum dosage, pH and contact time were obtained to be 0.01 g, pH 2 and 20 min, respectively. Isotherm modeling revealed that the Freundlich equation could better describe the adsorption of RB4 dye onto the LSMO as compared to other models. Kinetic data were appropriately fitted with the pseudo-secend-order adsorption rates. Based on the high specific surface area and nano-scale particle size, LSMO indicated favorable adsorption behavior for RB4 dye. Moreover, the adsorbent displayed a good specific efficiency for removal of RB4 dye in natural waters. In the future using other synthesis methods such as hydrothermal, combustion gel, etc. for

preparation of nanopowders according to their application. Also removal of environmental pollutants such as pharmaceutical and biological pollutants by perovskite will investigate.

References

[1] L.G. Tejuca, J.L.G. Fiero, New York (1993).

[2] M.Yazdanbakhsh , H. Tavakkoli, *Desalination*, 281,388 (2011).

[3] H. Jeong, T. Kim, D. Kim, K. Kim,*Int. J. Hyd. Energy*, 31, 1142 (2006).

[4] M .Carbajo, F.J. Beltran, F. Medina, O. Gimeno, F.J. Rivas,*Appl. Catal. B: Environ*., 67, 177 (2006).

[5] M.Siddique, R.Farooq, A.Khalid, A. Farooq, Q.Mahmood, U.Farooq,I. A.Raja, S. F. Shaukat, *J. Hazard. Mater*.,172, 1007 (2009).

[6] A.R.Tehrani , N.M.Mahmoodi , *Desalination*, 260,34 (2010).

[7] Y.Wong, J .Yu. *Water Res*.,33, 3512 (1999).

[8] H. Tavakkoli, F. Hamedi, *Res. Chem. Intermed*., 42, 3005, (2016).

[9] R .Wu, J. Qu, H .He, Y. Yu., *Appl. Catal. B: Environ.,* 48, 49(2004).

[10] D.M. Indra, C.S. Vimal, K.A. Nitin, *Dyes Pig.,* 69, 210 (2006).

[11] P.N. Kuznetsov, L.I. Kuznetzova, A.M. Zhyzhaev, G.L. Pashkov, V.V. Boldyrev, *Appl. Catal. A: General*, 227, 299 (2002).

[12] J. Kim, I.Honma, *Electrochim. Acta*, 49, 3179(2004).

[13] S. Lui, X. Qian, J. Xiiao, *J. Sol-Gel Sci. Tech.*, 44, 187 (2007).

[14] K. Nakamoto, Plenum Press, New York (1978).

[15] Y.S. Al-Degs, M.I. El-Barghouthi, A.H. El-Sheikh, G.M. Walker, *Dyes Pig.,* 77, 16 (2008).

[16] E. Erdem, G. Colgecen, R. Donat, *J. Colloid. Interf. Sci*.,282, 314 (2005).

[17] X. Wang, N. Zhu, B. Yin, *J. Hazard. Mater.,* 153, 22 (2008).

[18] G. Moussavi, M. Mahmoudi, *J. Hazard. Mater.,* 168, 806 (2009).

[19] S. Song, L. Xu, Z. He, H. Ying, J. Chen, X. Xiao, B. Yan, *J. Hazard. Mater*.,152, 1301 (2008).

[20] J.Z. Kong, A.D. Li, H.F. Zhai, H. Li, Q.Y. Yan, J. Ma, D. Wu, *J. Hazard. Mater.,* 171, 918. (2009)

[21] G. Zhang, J. Gong, X. Zou, F. He, H. Zhang, Q. Zhang, Y. Liu, X. Yang, B. Hu, *J. Chem. Eng.*,123, 59 (2006).

[22] S.C.R. Santos, V.J.P. Vilar, R.A.R. Boaventura, *J. Hazard.Mater.*,153, 999 (2008).

[23] Y. S. Ho, G. McKay, *Process Biochem*., 34, 451 (1999).

[24] A. Afkhami, R. Moosavi, *J. Hazard. Mater*., 174, 398 (2010).

[25] I. Langmuir, *J.Amr. Chem. Soc.,* 40, 1361 (1918).

[26] H.M.F. Freundlich, *Z. Phys. Chem.* A, 57, 3859(1906).

[27] X.C. Fu, W.X. Shen, T. Y. Yao, Physical Chemistry (Fourth edition), Higher Education Press, China, 303 (1994).